Towards ultrathin fiber-optic probe for simultaneous photoacoustic and fluorescence endoscopy

Tianrui Zhao
School of Biomedical Engineering and Imaging Sciences
King's College London
London, UK
tianrui.zhao@kcl.ac.uk

Michelle T. Ma
School of Biomedical Engineering and Imaging Sciences
King's College London
London, UK
michelle.ma@kcl.ac.uk

Sebastien Ourselin
School of Biomedical Engineering and Imaging Sciences
King's College London
London, UK
sebastien.ourselin@kcl.ac.uk

Tom Vercauteren
School of Biomedical Engineering and Imaging Sciences
King's College London
London, UK
tom.vercauteren@kcl.ac.uk

Wenfeng Xia
School of Biomedical Engineering and Imaging Sciences
King's College London
London, UK
wenfeng.xia@kcl.ac.uk

***Abstract*— A dual-modal photoacoustic and fluorescence endoscopy probe based on a single multimode fiber with a diameter of 140 μm was developed. By using a digital micromirror device with a high-speed algorithm for modulating the incident optical wavefront, the light transmission distortion through a multimode fiber was characterized and thus a focused laser beam was scanned at the distal fiber tip for microscopy imaging. Evaluation of the imaging performance was conducted with a dual-modal phantom comprising carbon fibers and fluorescence beads, and mouse red blood cells. The imaging probe has the potential to be further miniaturized using a fiber-optic ultrasound sensor so that it could be integrated into surgical tools such as medical needles for the guidance of minimally invasive procedures.**

Keywords—Photoacoustic imaging, fluorescence imaging, wavefront shaping

I. Introduction

Endoscopes have been widely used for the visualization of internal tissue *in sit*u, however, conventional endoscopes only provide morphological information of superficial tissue. Thus, endoscopes that can provide structural, molecular, and functional information of tissue at high-spatial resolution in real-time have long been a goal [1]. Several imaging modalities have been developed for endoscopic imaging over the last two decades. Optical coherence tomography can provide 3D high-resolution images of tissue structural information based on optical scattering of tissue, but it is challenging to achieve functional information such as blood oxygen saturation. Fluorescence and confocal micro-endoscopy provide molecular contrast but are limited in their capability to achieve depth information.

Photoacoustic (PA) imaging is a hybrid biomedical imaging modality capable of distinguishing spectroscopic signatures of tissues with high spatial resolution and large penetration depth. With PA imaging, tissue chromophores convert light energy into transient local temperature rise under pulsed or intensity-modulated light illumination, leading to the generation of ultrasound waves, which are then received by ultrasound detectors to form images of tissue optical absorption. As such, rich optical contrast is encoded into PA images by detecting the optically excited, depth-resolved ultrasound signals [2-5]. In the past decade, various minimally invasive photoacoustic imaging systems have been studied to extend PA imaging applications to examining deep internal tissues [4]. While more attention was paid to the development of side-viewing photoacoustic endoscopes, forward-viewing photoacoustic probes, which are more suitable for some surgical and interventional applications, were relatively less researched [6,7]. Coherent fiber bundles comprising a large number of individual fiber cores are commonly used for endoscopy, where each core in the bundle is equivalent to an image pixel [8]. They have been used for developing forward-viewing PA and fluorescence imaging probes by focusing light through individual cores to generate ultrasound waves and fluorescence light from imaging targets at the distal bundle tip. So, PA and fluorescence microscopy images can be achieved by spatially scanning the excitation lasers at the proximal end of the fiber bundle. The lateral spatial resolution with this configuration is determined by the spacing between each core (e.g. ~7 μm) [8]. Recently, it is reported that the miniaturization of a dichromatic Fabry-Perot ultrasound sensor deposited at a fiber bundle tip enabled PA tomography at the distal end of the fiber bundle. Here each core of the fiber bundle essentially served as an ultrasound detector element in PA tomography. However, for the guidance of minimally invasive procedures such as brain surgery, a thinner probe allowing the integration with medical needles is desired. Recently, multimode fibers (MMFs) with an outer diameter of around 100 μm allowing endoscopy with an optical diffraction-limited spatial resolution have been studied as an alternative of fiber bundles. With the development of wavefront shaping, the disordered light transmission caused by mode dispersion and coupling can be utilized to scan a focused laser beam at the distal fiber tip for microscopic imaging [11,12], allowing several through-MMF imaging modalities such as fluorescence [13], two-photons [14], Raman [15] and PA imaging [16]. The combination of two modalities, PA and fluorescence imaging, was also achieved, however, the use of liquid-crystal spatial light modulator for light modulation limited the imaging speed of MMF-based PA imaging to 30 s for the acquisition of a single image frame [17].

This project was supported by the Academy of Medical Sciences/the Wellcome Trust/ the Government Department of Business, Energy and Industrial Strategy/the British Heart Foundation/Diabetes UK Springboard Award [SBF006/1136], Wellcome Trust (203148/Z/16/Z, WT101957) and Engineering and Physical Sciences Research Council (NS/A000027/1, NS/A000049/1).

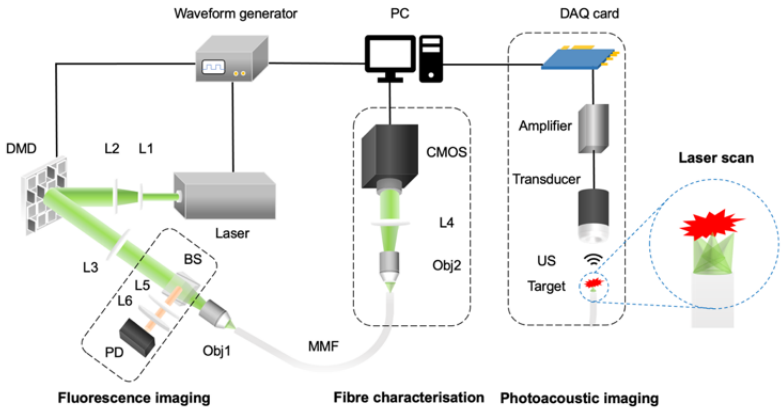

Fig. 1. Experimental setup of the imaging system. DMD: digital micromirror device; CP, circular polariser; L1,tube lens (f = 30 mm); L2, tube lens (f = 50 mm); L3-5, tube lenses (f = 100 mm); L6, dichroic mirror (longpass Filter, cut-on wavelength: 550 nm); BS, beam splitter; CMOS: complementary metal-oxide-semiconductor camera; US, ultrasound; PD: Photodetector; UST, ultrasound transducer; Obj1-2: Objective lenses; MMF, multimode fiber; DAQ, data acquisition.

In this work, we employed a high-speed digital micromirror device (DMD) for light modulation and developed a dual-modal PA and fluorescence imaging probe based on MMFs with a scanning speed two orders of magnitude higher than the studies in the literature [16, 17]. A real-valued intensity transmission matrix (RVITM) algorithm [18-20] was used for characterizing laser transmission and then generating optimal DMD patterns to focus laser through MMFs. PA images of mouse red blood cells (RBCs) were achieved with high fidelity, and dual-modal imaging with both PA and fluorescence imaging was simultaneously achieved with phantoms comprising of carbon fibers and fluorescent microspheres.

II. Methods

A. *Focusing light through MMFs with the RVITM algorithm*

In our previous study, we developed the RVITM method for image transmission and coherent light focusing through MMFs by characterizing the light intensity changes through the fibers [18,20]. Briefly, a series of binary patterns [H_1, H_2] were displayed by DMD as input whilst the corresponding output speckles at the distal fiber tip were recorded. Here a Hadamard matrix H ∈ (-1, +1) with dimensions of N × N was firstly generated and then converted into two binary matrices $H_1 = (H + 1)/2$ and $H_2 = (-H + 1)/2$. Then, the light intensity changes from input to output are approximately expressed as:

$$\begin{bmatrix} I_1^1 & \cdots & I_1^p \\ \vdots & \ddots & \vdots \\ I_m^1 & \cdots & I_m^p \end{bmatrix} = RVITM \cdot \left[H_1, H_2\right],$$

where $I^p{}_m$ is the intensity at the m^{th} output mode when the p^{th} input binary pattern is displayed. The value of RVITM can be calculated via matrix manipulation:

$$RVITM = \begin{bmatrix} 2I_1^1 - I_1^1 & \cdots & 2I_1^p - I_1^1 \\ \vdots & \ddots & \vdots \\ 2I_m^1 - I_m^1 & \cdots & 2I_m^p - I_m^1 \end{bmatrix} \cdot [H, -H]^T,$$

where [H, -H] ^{T} is the transpose of [H, -H] and [H, -H] ^{T} = [H, -H]$^{-1}$ owing to the Hadamard matrix properties. As a result, the value of RVITM characterized the intensity change at each output mode when one micromirror is switched 'ON'; when the value of an RVITM element is larger than 0, switching 'ON' the corresponding micromirror can improve the light intensity at the corresponding output mode. So, optimal DMD patterns for light focusing and scanning through the fiber can be obtained by switching 'ON' micromirrors with a higher RVITM value than 0. In addition, we also experimentally demonstrated that a preset threshold for determining 'ON' micromirrors can be used to further improve the focusing quality, which is detailed in reference [17].

B. *Experimental setup and imaging*

A schematic diagram of the experimental setup is shown in Fig. 1. A 532 nm laser with a pulse duration of 2 ns (SPOT-10-200-532) was reflected by a DMD (DLP7000) to project binary patterns onto the proximal end of an MMF via a tube lens (AC254-050-A-ML, Thorlabs) and an objective (20×, RMS20X, Thorlabs). Here different fibers were studied for PAI including a Ø62.5 μm, 0.275 NA, gradient-index (GRIN) fiber from Thorlabs, a Ø100 μm, 0.29 NA GRIN fiber from Newport, and a Ø200 μm, 0.22 NA step-index fiber from Thorlabs. A sub-region of 128 × 128 micromirrors was used for light modulation. In front of the distal fiber tip, a CMOS camera (C11440-22CU01, Hamamatsu Photonics) was used to capture the output speckles after an objective (20×, RMS20X, Thorlabs) and a tube lens (AC254-0100-A-ML, Thorlabs). After the RVITM characterization, the characterization module was removed, and the imaging samples were placed at the optical focal plane and a focused ultrasound transducer (50 MHz, V358) was used for detecting PA signals. The MMF also collected excited fluorescence signals and these signals were detected by a photodetector via a beam splitter, a concave lens, and a bandpass filter. Then PA and fluorescence signals were amplified and digitized for

images formation. Each image comprised 100×100 pixels and the scanning step was set to be 0.5 μm. Synchronization of the laser pulsing, data acquisition, and DMD display was controlled by a waveform generator (33600A, Keysight, Santa Rosa) and a customized MATLAB program.

III. Results

A. Photoacoustic imaging of carbon fibers

After the fiber characterization, tightly focused light spots were achieved in front of the distal MMF tip with a core diameter of ~ 100 μm. The diameters of the light foci were measured to be around 1.5 μm and the light intensity at the focusing pixel is ~ 1200 times higher than the intensity in the background. By scanning the focused laser spot and detecting the excited ultrasound from a phantom comprising carbon fibers, PA imaging was achieved through different MMFs as shown in Fig. 2. The lateral spatial resolution was measured to be ~ 1.7 μm. PA images were displayed with maximum intensity projections along the depth direction. The structures of the carbon fiber networks were clearly visualized with PA images with a high consistency to the corresponding optical microscopy images. Furthermore, the individual carbons in the overlapped regions were not distinguished in the optical microscopy images and were visualized with clear boundaries in PA imaging.

B. Photoacoustic imaging of mouse RBCs

The performance of the imaging probe was further evaluated by imaging mouse RBCs as shown in Fig. 3. The bi-concave structures of RBCs were clearly visualized with PA imaging and corresponded well to the optical microscopy images of the samples over the same field-of-view. As the

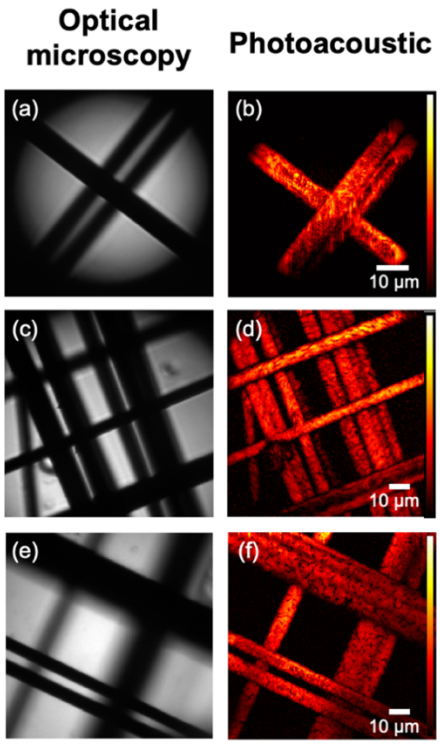

Fig. 2. Photoacoustic imaging of carbon fibers through (b) a Ø62.5 μm, 0.275 NA GRIN multimode fibers, (d) a Ø100 μm, 0.29 NA GRIN fiber and (f) a Ø200 μm, 0.22 NA step-index fiber.

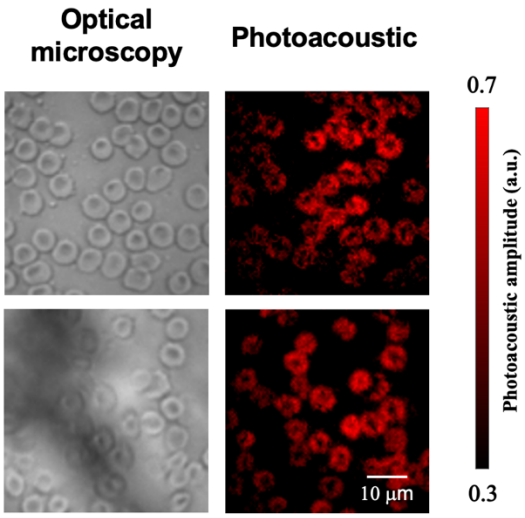

Fig. 3. Photoacoustic imaging of mouse red blood cells.

DMD was running at 22.7 kHz, the rate of image acquisition was 2.27 frames per second (fps) for 10000-pixels images. However, here the PA signals were averaged by 16 times over sequential measurements to achieve high signal-to-noise-ratios when imaging RBCs, reducing the imaging speed by 16 times. This issue is likely to be solved by employing a higher power laser as the excitation source.

C. Simultaneous photoacoustic and fluorescence imaging

Simultaneous dual-modal imaging was achieved by imaging a phantom comprising of a carbon fiber and 4-μm fluorescent microspheres. As shown in Fig. 4, PA images visualized the carbon fiber with high fidelity, and fluorescence imaging highlighted the fluorescent microspheres as expected, which corresponded well to the corresponding optical microscopy images.

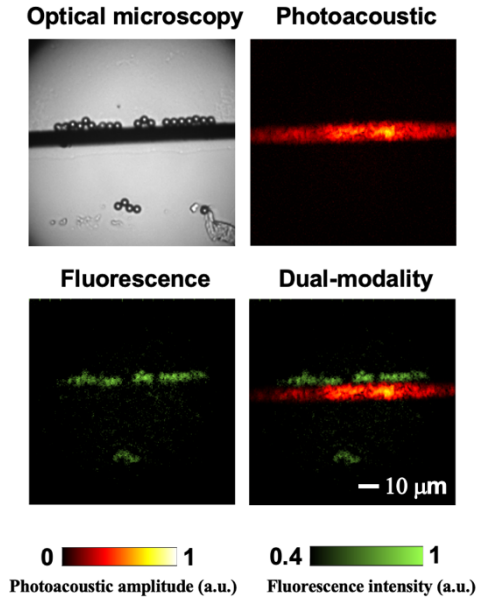

Fig. 4. Dual-modal photoacoustic and fluorescence imaging of carbon fibers and fluorescent microspheres.

IV. Discussion

In this work, we developed a dual-modal imaging probe for PAI and fluorescence imaging simultaneously. With the use of a high-speed DMD for modulating the incident laser, a focused laser beam was scanned in front of the distal fiber tip for the formation of microscopy images in both PA and fluorescence modes. The capability of PA imaging was demonstrated with both carbon fiber phantoms and mouse RBCs *ex vivo*, whilst dual-modal imaging was demonstrated with a phantom comprising a carbon fiber and fluorescent microspheres. Compared with forward-viewing PA endoscopes based on fiber bundles, our imaging probe benefits a higher spatial resolution of ~1.7 μm defined by optical diffraction, and an ultrathin size of 140 μm in fiber diameter. The DMD was operated at a rate of 22.7 kHz, meaning that 22.7 k pixels can be formed per second, enabling a frame rate of 2.27 fps for the acquisition of an image covering an area of 50 μm × 50 μm with a 0.5 μm scanning step. In comparison, it took 30 s to acquire a PA image with the liquid crystal spatial light modulator-based system [17].

Since the implementation of microscopy imaging relies on the characterization of light transmission through MMFs, significant geometry changes of MMFs can lead to the degradation of focusing quality, so the fibers were kept stationary during the imaging experiments in this study. In a recent study, it was reported that GRIN fibers have a high resistance to geometry changes on the imaging performance [21]. In future, the imaging performance of our GRIN fibers-based system will be investigated with fiber bending.

V. Conclusion

In summary, we developed a dual-modal PA and fluorescence endo-microscopy probe based on MMFs. With a fast DMD used for wavefront shaping, high-fidelity PA images of carbon fibers and mouse RBCs were acquired at high speed and dual-modality imaging capability was demonstrated with phantoms consisting of carbon fibers and fluorescence microspheres.

Acknowledgment

We thank Dr. Cinzia Imberti, Dr. Charlotte Rivas, and Dr. Truc Pham from King's College London for helping with collecting mouse blood, and Mr. Keith Oakes from Elforlight Ltd. for technical support on the excitation laser.

References

[1] T. Wang and J. Van Dam, Optical biopsy: a new frontier in endoscopic detection and diagnosis, *Clinical gastroenterology and hepatology*, *2* (2004) 744-753.

[2] P. Beard, Biomedical photoacoustic imaging, Interface Focus 1 (2011) 602–631.

[3] Y. Zhou, J. Yao, L.V. Wang, Tutorial on photoacoustic tomography, J. Biomed. Opt. 21 (2016) 061007.

[4] T. Zhao, A.E. Desjardins, S. Ourselin, T. Vercauteren and W. Xia, Minimally invasive photoacoustic imaging: Current status and future perspectives, *Photoacoustics*, *16* (2019) 100146.

[5] J. Joseph, M.R. Tomaszewski, I. Quiros-Gonzalez, J. Weber, J. Brunker and S.E. Bohndiek, Evaluation of precision in optoacoustic tomography for preclinical imaging in living subjects. *Journal of Nuclear Medicine*, *58* (2017), 807-814.

[6] K. Jansen, A.F.W. van der Steen, H.M.M. van Beusekom, J.W. Oosterhuis, G. van Soest, Intravascular photoacoustic imaging of human coronary atherosclerosis, Opt. Lett. 36 (2011) 597–599.

[7] S.J. Mathews, C. Little, C.D. Loder, R.D. Rakhit, W. Xia, E.Z. Zhang, P.C. Beard, M.C. Finlay, A.E. Desjardins, All-optical dual photoacoustic and optical coherence tomography intravascular probe, Photoacoustics 11 (2018) 65–70.

[8] P. Shao, W. Shi, P.H. Reza, R.J. Zemp, Integrated micro-endoscopy system for simultaneous fluorescence and optical-resolution photoacoustic imaging, J. Biomed. Opt. 17 (2012) 076024.

[9] R. Ansari, E.Z. Zhang, A.E. Desjardins, P.C. Beard, All-optical forward-viewing photoacoustic probe for high-resolution 3D endoscopy, Light Sci. Appl. 7 (2018) 75.

[10] E.J. Alles, N.F. Sheung, S. Noimark, S., E.Z. Zhang, P.C. Beard and A.E. Desjardins, A reconfigurable all-optical ultrasound transducer array for 3D endoscopic imaging. *Scientific reports*, *7* (2017), 1-9.

[11] T. Čižmár and K. Dholakia, Shaping the light transmission through a multimode optical fiber: complex transformation analysis and applications in biophotonics, Opt. Express 19 (2011), 18871–18884.

[12] I. N. Papadopoulos, S. Farahi, C. Moser, and D. Psaltis, Focusing and scanning light through a multimode optical fiber using digital phase conjugation, Opt. Express 20 (2012) 10583–10590.

[13] S. Turtaev, I. T. Leite, T. Altwegg-Boussac, J. M. Pakan, N. L. Rochefort, and T. Čižmár, High-fidelity multimode fiber-based endoscopy for deep brain in vivo imaging, Light: Sci. Appl. 7 (2018) 92–98.

[14] E. E. Morales-Delgado, D. Psaltis, and C. Moser, Two-photon imaging through a multimode fiber, Opt. Express 23 (2015) 32158–32170.

[15] I. Gusachenko, M. Chen, and K. Dholakia, Raman imaging through a single multimode fiber, Opt. Express 25 (2017) 13782–13798.

[16] I. N. Papadopoulos, O. Simandoux, S. Farahi, J. Pierre Huignard, E. Bossy, D. Psaltis, and C. Moser, Optical-resolution photoacoustic microscopy by use of a multimode fiber, Appl. Phys. Lett. 102 (2013) 211106.

[17] S. Mezil, A. M. Caravaca-Aguirre, E. Z. Zhang, P. Moreau, I. Wang, P. C. Beard, and E. Bossy, Single-shot hybrid photoacoustic-fluorescent microendoscopy through a multimode fiber with wavefront shaping, Biomed. Opt. Express 11 (2020), 5717–5727.

[18] T. Zhao, S. Ourselin, T. Vercauteren, and W. Xia, Seeing through multimode fibers with real-valued intensity transmission matrices, Opt. Express 28 (2020), 20978–20991.

[19] T. Zhao, S. Ourselin, T. Vercauteren, and W. Xia, High-speed photoacoustic-guided wavefront shaping for focusing light in scattering media, Opt. Lett. 46 (2021), 1165–1168.

[20] T. Zhao, S. Ourselin, T. Vercauteren and W. Xia, Focusing light through multimode fibers using a digital micromirror device: a comparison study of non-holographic approaches, Opt. Express, 29 (2021), 14269-14281.

[21] D. E. B. Flaes, J. Stopka, S. Turtaev, et al., Robustness of light-transport processes to bend-ing deformations in graded-index multimode waveguides, Physical review letters 120 (2018) 233901.